Applied Clay Science 238 (2023) 106930

Contents lists available at ScienceDirect

Applied Clay Science

journal homepage: www.elsevier.com/locate/clay

Research Paper

Halloysite nanotubes/Keratin composites for wool treatment

Maria Rita Caruso, Giuseppe Cavallaro *, Stefana Milioto, Giuseppe Lazzara

Dipartimento di Fisica e Chimica Emilio Segrè, Università degli Studi di Palermo, Viale delle Scienze, pad. 17, 90128 Palermo, Italy

ARTICLE INFO

Keywords:
Keratin
Halloysite nanotubes
Nanocomposite
Wool treatment
DMA
Colorimetry
Cultural heritage

ABSTRACT

The optimization of a consolidation and protection coating for wool-based artefacts is a challenging issue for conservator of cultural heritage. In this study, an aqueous dispersion containing Keratin (K) and Halloysite nanotubes (Hal) was investigated in a coating protocol for wool thread. Colorimetric analysis and optical microscopy revealed the surface characteristic of wool. Scanning electron microscope showed the halloysite nanotubes distribution in the wool fibers. The protection efficacy after UV-irradiation was evaluated and the mechanical analysis gave us direct information on consolidation and protection effect of Hal/K mixtures in treated wool thread samples. The formulation with the optimal performances was used on conservation protocol for a historical yarn. The obtained results indicate that the proposed protocol is promising to generate a reinforcing coating layer onto wool-based yarn also providing protection from deterioration due to UV exposure with a minimal impact on the sample aesthetic aspects.

1. Introduction

Aging process of artworks are the cause of conservation issues on cultural heritage. Natural and artificial materials undergo to chemical structure modification upon time and, irreversible changes in the aspect and physico-chemical properties may occur. Environmental condition such as temperature, humidity, pollutant and UV irradiation could affect the degradation process by speeding-up the material alteration generating a valuable impact on the fruition of the artwork itself.

Cellulose- and protein-based materials are among the most common materials of interest for scientist involved in the development of consolidation protocols because wood and natural fibers are widely used as decorative objects. Aging effects typically generates a loss of material that needs a proper treatment to keep the physico-chemical features at least unaltered from further stress in the future (Giorgi et al., 2002; Chen et al., 2018; Lisuzzo et al., 2021b, 2021c; Dei et al., 2023).

Wool is obtained from the hairy covering of sheep or goats and it is among most commonly used animal fiber in historical textiles. Keratin is the main constituent of wool and due to the presence of histidine, tryptophan and tyrosine in its backbone, UV radiation can induce photodegradation of the fiber (Degano et al., 2011). Clay minerals are known for their UV-protection ability in several application (Hoang-Minh et al., 2010). Modified clay minerals have been immobilized onto textiles to generate functional products with high added-value (Monteiro et al., 2014).

In the last two decades, researchers paid more attention on sustainable material for the conservation of artwork. Biopolymers (mainly protein and carbohydrates), natural nanomaterials (nanoclays among all) and essential oils have been investigated in several protocols to improve physico-chemical performances and efficacy of formulations for consolidation, protection and cleaning treatments (Cavallaro et al., 2019, 2020b; Baglioni et al., 2021; Samal and Blanco, 2021; Alcalá et al., 2022; Pramualkijja and Jiratumnukul, 2022; Dei et al., 2023).

Due to chemical characteristics, biocompatibility and reduced costs, the use of keratin/clay composites have been exploited in tissue engineering (Giannelli et al., 2021), human hair treatments (Cavallaro et al., 2020a, 2022), water decontamination (Zhang et al., 2021) and it can be promising in conservation of wool-based artworks.

Among clay minerals, Halloysite nanotubes (Hal) have been investigated in conservation protocols for cultural heritage thanks also to their ability to get dispersed uniformly in the solution and performance as filler for several kind of organic matrixes (Gorrasi et al., 2018; Yu et al., 2019; Bertolino et al., 2020; Zhao et al., 2020). Just to quote some relevant field of applications, Halloysite nanotubes can be used as reinforcing agent of scaffolds for tissue engineering (Liu et al., 2013; Fakhrullin and Lvov, 2016; Gkouma et al., 2021; Wong et al., 2023), composite materials for biomedical applications (Feng et al., 2022, 2023), bioplastics for packaging (Aghajani-Memar et al., 2022; Boccalon et al., 2022), decontamination purposes (Yang et al., 2021), catalysis (Liu et al., 2018; Sadjadi et al., 2018; Feng et al., 2020; Sadjadi, 2020)

* Corresponding author.
E-mail address: giuseppe.cavallaro@unipa.it (G. Cavallaro).

https://doi.org/10.1016/j.clay.2023.106930
Received 30 January 2023; Received in revised form 10 March 2023; Accepted 25 March 2023
Available online 3 April 2023

and emulsion stabilizer on dispersion for developing a new material for cultural heritage (Lisuzzo et al., 2021a).

In this work, we studied the combination of halloysite nanotubes with keratin to obtain green nanocomposite materials as a coating layer for the treatment of wool samples.

Keratin can be incorporated within the wool thread and be cross-linked through disulphide bonds reducing the aging effects. Hal, as nanofiller, enhances the consolidation efficiency of dispersion, can play an active role in physico-chemical properties such as photochemical sensitivity, tensile performances and it can open further route for a longer-term action by incorporating active species for a slow release. Besides the tests on contemporary wool, the proposed protocol was applied on a yarn sample from an historical tapestry.

2. Experimental section

2.1. Materials

Hydrolyzed Keratin (K) was gift from Kelisema srl and it is obtained from hair of sheep. Halloysite nanotubes, Hals ($Al_2Si_2O_5(OH)_4{\cdot}2H_2O$), were a gift from I-Minerals Inc. The composition of Hal is 90% of halloysite with about 9.5% of kaolinite and 0.5% of quartz. The XRD pattern of Hal is provided in supporting information. Wool samples were 100% pure sheep Merinos. Historical yarn, wool based, was from a Flemish tapestry of the sixteenth century from an unknown artist (it belongs to the Tapestry Museum of Marsala in Sicily, Italy).

2.2. Preparation of halloysite dispersions in keratin aqueous solution

Keratin solutions were prepared at 1 mass% of concentration, by magnetic stirring for 1 h at 25 °C. Halloysite nanotubes at variable concentration, from 0% to 1%, were added in the keratin solution. The dispersions were sonicated for 10 min and magnetically stirred overnight at 25 °C. The Hal/K mass ratio ($R_{Hal:K}$) was varied from 0 to 10.

2.3. Wool treatment by immersion within the Hal/K dispersion

An immersion protocol was carried out to compare different Hal/K dispersion on wool treatment. Samples were washed with water to and then they were immersed into Eppendorf with Hal/K dispersion at 25 °C on the basculator for 15 and 60 min. The wool samples were dried and stored in controlled relative humidity (75 ± 1%) and temperature (25 ± 0.1 °C).

2.4. Aging of wool samples by UV irradiation exposure

UV-radiation was performed to carry out aging test on untreated wool and treated wool with Hal/K dispersion. Samples were exposed to irradiation of 500 Wm^{-2} for 1 week under controlled temperature (25 ± 0.1 °C) and relative humidity (75 ± 1%) of the room.

3. Methods

3.1. Optical microscope

The optical micrographs were taken with an Optika polarizing microscope at room temperature, and the images were acquired at 4×/0.10, 10×/0.25 and 40×/0.65 objectives magnification.

3.2. Colorimetric analysis

Colour parameters of treated and untreated wool samples were measured using a colorimeter (NH300 Colorimeter, 3NH Shanghai Co., Ltd.) with a spot size of 8 mm. The device was calibrated using black and white plates. CQCS3 Software was used for data acquisition, a* (red-green), L* (lightness), and b* (yellow-blue) parameters, whiteness index (WI), yellowness index (YI) and total colour differences (ΔE) are measured for each treated wool samples and compared to untreated wool by using the following equations:

$$YI = 142.86\ (b^*/L^*) \tag{1}$$

$$WI = 100{-}\sqrt{\left[(100{-}L^*)^2 + a^{*2} + b^{*2}\right]} \tag{2}$$

$$\Delta E = \sqrt{\left[(L^* - L_0{}^*)^2 + (a^* - a_0{}^*)^2 + (b^* - b_0{}^*)^2\right]} \tag{3}$$

3.3. Scanning Electron Microscopy (SEM)

SEM microscope (Desktop SEM Phenom PRO X PHENOM) was used to investigate of morphological characteristic of treated wool samples. The energy of beam ranged between 4.8 and 20.5 kV. Each sample was preliminarily coated with gold to avoid charging effects under an electron beam.

3.4. Dynamic Mechanical Analysis (DMA)

Tensile properties of untreated and treated wool sample were evaluated by a Dynamic Mechanical Analysis (DMA) Q800 apparatus (TA Instruments). The experiment was carried out under a controlled force of stress ramp of 10 MPa / min^{-1} at 25.0 ± 0.5 °C. Universal Analysis software (TA Instruments) allowed us to analyse stress vs strain curves and to determine mechanical performances in terms of yield tensile strength, maximum elongation, stress at breaking point and Young's modulus at the sample fracture.

3.5. X-ray Diffraction (XRD)

The patterns were obtained from an X-ray diffractometer (Rigaku, MiniFlex) with a CuKa radiation source including a nickel filter and working at 40 kV and 15 mA. The wavelength of the X-ray beam was 1.5406 Å, and the layer spacing of the samples was calculated by the and Bragg's equation, which can be expressed as.

$$n\lambda = 2\mathrm{dsin}\ \vartheta \tag{4}$$

where θ is the angle that the outgoing beam forms with the crystalline layer, λ is the wavelength of the radiation, d is the distance between two adjacent layers and n can be 1,2 or 3.

The angle for scanning was ranged from 2° to 70° with a rate of 20° min − 1 and a step of 0.02°.

3.6. ζ-potential

ζ-potential measurements were performed by Zetasizer Nano-ZS (Malvern Instruments) under isothermal conditions. Specifically, the temperature was set at 25 °C. The experiments were conducted using disposable folded capillary cell was used.

4. Results and discussion

4.1. Preparation and surface characteristics of Hal/K dispersion on wool samples

A series of Hal/K dispersion in water was prepared from a stock solution of keratin (K) at constant concentration (1 mass%) by adding variable Hal amounts in the range from 0.1 mass% to 1 mass%. The mass ratio between Hal and K is indicated as $R_{Hal:K}$. The Hal/K aqueous dispersions exhibited a high colloidal stability in agreement with their ζ potential values, which range between −39 and − 43 mV. Accordingly, halloysite nanotubes are stable in water because of the electrostatic repulsions. We observed that the Hal/K dispersions are stable for 12 h at least, whilst a nanotubes sedimentation is observed for the bare Hal in 2 h from preparation. These results are in agreement with turbidimetric

reports (Cavallaro et al., 2020a). The stabilization of the colloidal dispersion at neutral pH is a consequence of the electrostatic interactions between Hal and keratin. In particular, the protein at pH above the isoelectric point (pI = 4.0) is adsorbed to the positively charged Hal lumen increasing the net charge of the nanotubes and therefore hindering the agglomeration and sedimentation process (Cavallaro et al., 2020a). The wool treatment protocol is based on the fiber immersion, and it is sketched in Fig. 1.

Wool thread samples were imaged with an optical microscope. Untreated wool thread (diameter of 0.12 mm) is characterized by many fibers (diameter of ca. 0.01 mm) twisted together (Fig. 2). The wool fibers present a cylindrical shape with a lumen and are covered with large scales overlapping on each other that gives wool the ability to felt (Fig. 2d). The wool thread exhibits a typical pattern without striations or damaged scales, confirming the status of the sample used in this study (Fig. 2c).

As concerns the treated wool samples, the optical microscope shows that Hal/K dispersion successfully covered the fibers (Figs. 2 and 3) although it did not produce any significant variations by eye observation. It should be noted that the dispersion covered each fibers without create a single stiff thread, so the mobility of fibers isn't compromised by the treatment as well as the general aspect (Figs. 2 and 3).

The deposition of Hal on wool samples was clearly visualized by using SEM, which evidenced that halloysite nanotubes are randomly positioned. The clay is deposited especially on scales of wool fibers as anchoring site. A similar result was observed for Hal deposited onto human hair that showed a nanotubes accumulation near the coticules (Panchal et al., 2018; Rahman et al., 2021).

The alteration of the aesthetic characteristic of the wool thread sample after the treatment can be assessed by measuring its optical properties and in particular the colour. The colorimetric data of wool yarns after each treatment were collected and compared with untreated wool sample (Table 1).

The colour change is calculated as total colour differences (ΔE) between standard sample and treated sample. The treatment with Hal/K dispersion does not alter the colour of the control surface, indeed, for human eyes, 2.3 is reported as a ΔE limit between undistinguished colours and the measured ΔE values are never above 1.4. Additionally, the white and yellow indexes (WI and YI in Table 1) revealed an unsubstantial deviation from the parameters of the untreated sample. Similar conclusions can be drawn by considering the CIELAB colour space diagram (see figure in Supporting informations) defined by the colour coordinate (L*, a* and b*). The experimental points are concentrated in a small region of the diagram confirming that the colour perception is unchanged after the treatment with Hal/halloysite dispersion compared to the control. Based on colorimetry results, Hal/K treatment doesn't alter aesthetical aspect of wool thread sample.

4.2. Strengthening effect of Hal/K dispersion on wool samples

The percentage of consolidant material (Hal/K) absorbed on wool samples (Consolidation %) was measured gravimetrically at two immersion times, 15 and 60 min. The coating efficiency doesn't depend on to immersion time of wool samples as the amount of absorbed material is varied within ±4% considering all of the investigated Hal/K compositions (see data in Supporting Information). The coating efficiency was estimated by gravimetric measurements. Therefore, a short-time treatment already ensures a wool fiber saturation with the Hal/K dispersion, due to the natural behaviour of wool thread to absorbs typically 20–30% of water inside fibers (Lo Nostro et al., 2002).

The effect of Hal/K composition on the consolidation can be evidenced by looking at the data obtained for an immersion time of 15 min. The keratin presence is necessary to improve the sticking of the consolidant material at the surface, in fact, the treatment with halloysite nanotubes dispersion has a low loading value (ca. 7%,). Fig. 4 shows the non-monotonic trend with a maximum for the consolidation % vs $R_{Hal:K}$ curve. The best consolidation performances are obtained for $R_{Hal:K} = 0.5$ being the adsorbed material two fold of the treatment with keratin dispersion. Above this composition, the addition of Hal in the Hal/K dispersion does not make any improvement in the consolidation efficacy most likely because keratin plays a key role in favouring the Hal sticking to the wool fiber and, in the presence of an excess of nanotubes, the consolidation % cannot be further increased.

A key aspect in the efficacy of the consolidation treatment is about the tensile properties of the sample. Mechanical analyses were conducted by measuring stress vs strain curves for wool thread samples

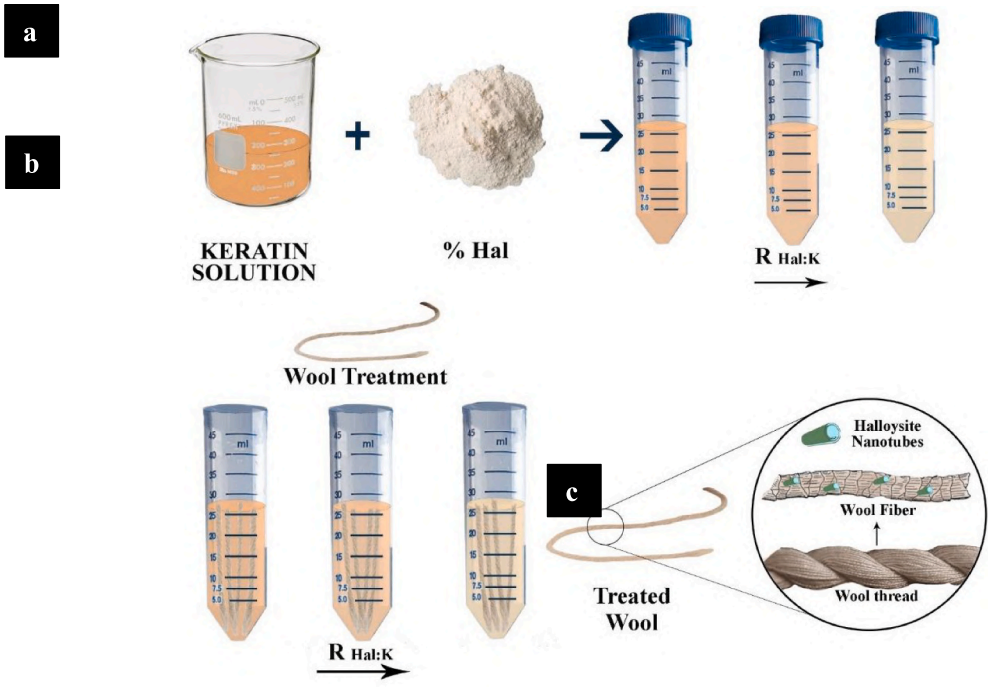

Fig. 1. Schematic representation of (a) the preparation of Hal/K dispersion; (b) the immersion protocol of wool samples and (c) the treated wool sketch.

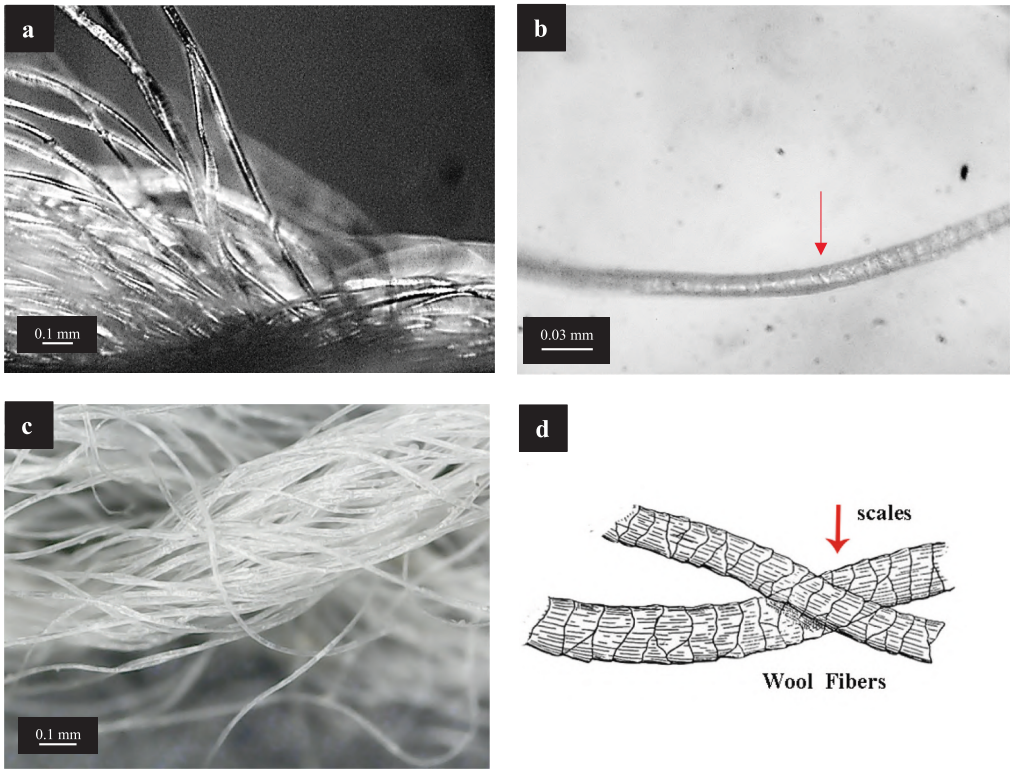

Fig. 2. Optical Microscope images of untreated wool thread sample at different magnification: (a) 10× image of untreated wool; (b) 40× image of wool fiber, scales are visible; (c) 2× image of treated wool thread with $R_{Hal:K} = 0.5$; (d) scheme of wool fibers where scales are marked with a red arrow. (For interpretation of the references to colour in this figure legend, the reader is referred to the web version of this article.)

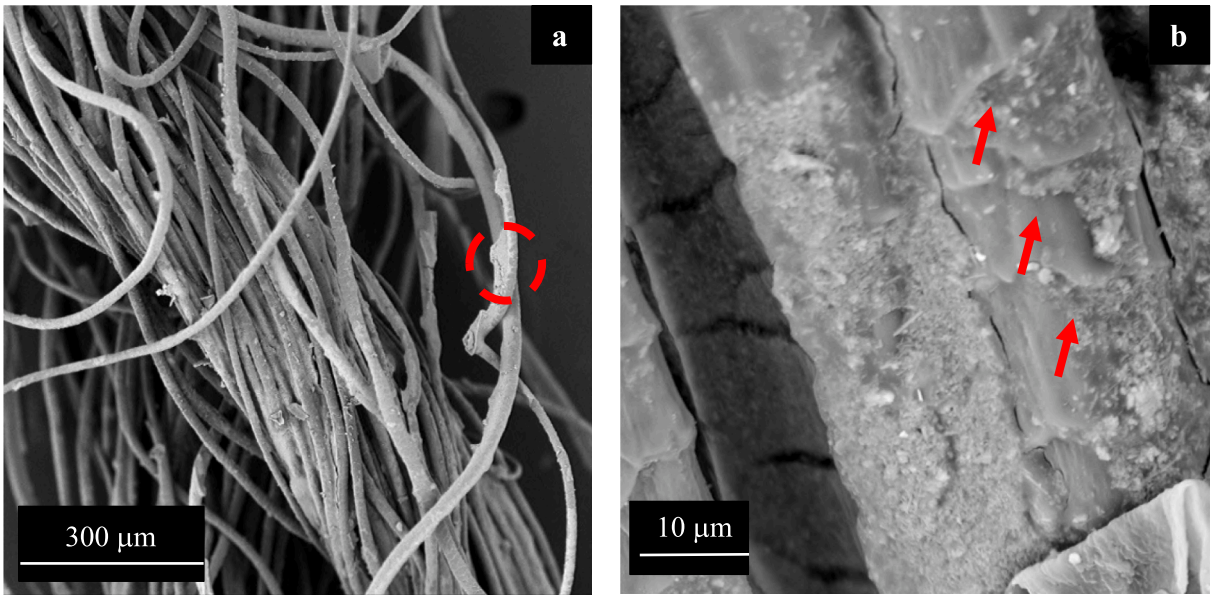

Fig. 3. Scanning Electron Microscopy images at different magnifications of treated wool sample ($R_{Hal:K} = 0.5$). Red circle indicates an example of Hal accumulation on the fibers, (a). Red arrows indicate scales of wool fibers with Hal accumulated, (b). (For interpretation of the references to colour in this figure legend, the reader is referred to the web version of this article.)

(Fig. 5).

Untreated wool sample display a Young Modulus of 2973 MPa that is lower than the values for all treated wool samples (See table in Supporting information). In agreement with the consolidation efficacy results, the best mechanical performances are achieved for the wool thread immersed in the mixture with $R_{Hal:K} = 0.5$. Namely, both the Young modulus and the stress at breaking (Fig. 5) have the maximum values in this circumstance.

The transition from an elastic region to a plastic region is defined by the yield point (%) that corresponds to the maximum deformation within an elastic regime. The proposed treatment protocol improved by a factor two the yield point of the wool yarn (see data in Supporting Information).

Finally, the consolidation treatment at $R_{Hal:K} = 0.5$ provided an

Table 1
Colorimetric parameters.*

Sample	L*	a*	b*	ΔE	WI	YI
Keratin	89.96	1.13	−1.41	**0.38**	76.7	−1.00
Hal	89.84	1.11	−1.63	**0.31**	78.62	−2.15
$R_{Hal:K} = 0.1$	89.51	1.29	−1.30	**0.21**	77.5	−1.33
$R_{Hal:K} = 0.25$	90.51	0.93	−1.74	**1.36**	80.26	−2.49
$R_{Hal:K} = 0.5$	89.15	1.40	−1.17	**0.57**	76.57	−0.97
$R_{Hal:K} = 0.75$	89.77	1.20	−1.36	**0.21**	78.12	−1.51
$R_{Hal:K} = 1$	89.07	1.49	−0.96	**0.79**	76.12	−0.47

* Control: untreated wool, L* = 89.60, a* = 1.24, b* = −1.48, WI = 77.92, YI = −1.74.

excellent efficiency in the adsorbed material and on mechanical performances, even if his maximum elongation is slightly lower than untreated wool sample.

The role of the immersion time on the mechanical properties of the wool treated with the mixture at $R_{Hal:K} = 0.5$ is negligible (Table 2) in agreement with the consolidation % data.

4.3. UV Protection of Hal/K dispersion on wool samples

Wool thread samples were exposed at UV irradiation for 1 week at room temperature and samples were observed with an optical microscope that evidenced the typical damage of wool fibers after aging (Vasileiadou et al., 2019). Namely, the high energy UV radiation induces structural changes on the surface of the fibers due to the presence of the aromatic amino acids residues that are photosensitive (Vasileiadou et al., 2019). As an example, Fig. 6 shows the sample treated with a Hal/K mixture ($R_{Hal:K} = 0.5$) where the tubular fibers appear crushed with an irregular shape after UV irradiation.

The protection's effect on wool thread samples was investigated by

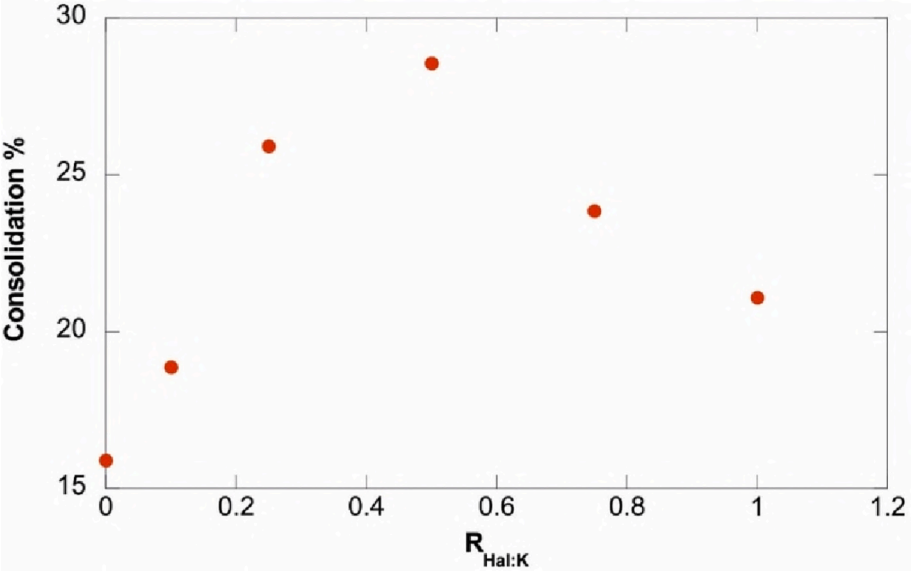

Fig. 4. Consolidation % of wool thread after 15 min immersion in Hal/K aqueous dispersions with variable composition.

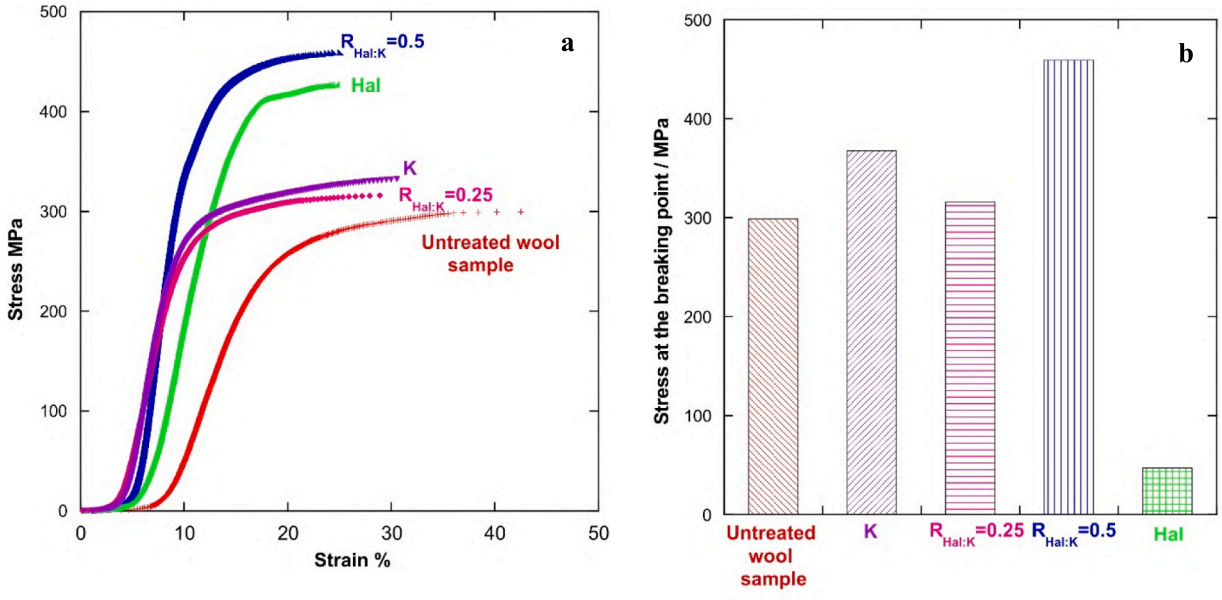

Fig. 5. (a) Stress vs Strain curves of native wool thread sample and after immersion in a Hal/K mixtures at different composition. (b) Stress at breaking of untreated and treated sample ($R_{Hal:K}$).

Table 2
Tensile Properties of Treated wool samples with Hal/K dispersion at variable immersion time.*

Time (minutes)	R Hal:K	Maximum Elongation (%)	Stress breaking point (MPa)	Yield Point (%)	Elastic Modulus (MPa)
15	0.5	25 ± 1.7	459 ± 32	10.6 ± 0.5	8530 ± 80
60	0.5	26.4 ± 1.8	439 ± 30	10.9 ± 0.5	7650 ± 74

* Control: Untreated wool sample max El.42.5%, Breaking point 299 MPa, Yield Point 18%, Elastic Modulus 2970 MPa.

comparing tensile properties before and after the UV irradiation. Fig. 7 compares the stress at breaking for wool yarns after UV irradiation. The treatment with Hal/K composites enhances the mechanical performances in all cases being $R_{Hal:K} = 0.5$ the optimal composition. It should be noted that Hal alone does not provide enough protection to the wool thread.

Hal/K treatment guaranteed a strong consolidation layer due to the capacity of Keratin to create a film with the chemical characteristics of the sample, and halloysite nanotubes increase mechanical resistance of wool sample. Both materials protect the wool thread from UV irradiation, according to data from DMA analysis where tensile properties were improved after aging samples. It should be noted that wool protective effect is caused by both halloysite, which increase the light reflectivity of the thread, and keratin that creates a UV-shielding layer.

4.4. Application of Hal/K treatment on Historical Yarn sample

Based on successful experimental findings on contemporary wool yarn, we considered to test the conservation protocol on a historical wool yarn by using a Hal/K dispersion with mass ratio $R_{Hal:K} = 0.5$. With this in mind, a sample of wool yarn from a Flemish tapestry dated back to the Sixteenth Century was considered. The extensive dynamic mechanical characterization on different coloured wool-based warp samples provided a clear evidence of a strong deterioration of the tensile properties compared to contemporary wool yarns (Caruso et al., 2022). The observation under optical microscopy showed that untreated historical yarn is characterized by wool-based fibers twisted together and with light brown colour (Fig. 8). An accumulation of deposited material on the fibers of the treated historical yarn was imaged by optical microscopy (Fig. 8), although the general morphological features and aspect by eye observation are not altered.

Tensile tests were carried out to assess the consolidation efficacy of Hal/K treatment. The stress vs strain curves (Fig. 9) evidence the different mechanical behaviour induced by the conservation protocol. The tensile parameters, provided in Table 3, indicate: an enhancement of ca. 15% of stress at breaking and an increasing of the yield point of ca. 35% and finally a maximum elongation ca. 65% larger due to the historical yarn treatment. Therefore, the treated sample can certainly dissipate more energy and stretch further before breaking. These results prove the efficacy of the protocol on naturally aged wool threads.

5. Conclusions

In this work, we proposed a novel treatment based on Halloysite nanotubes and Keratin (Hal/K) mixtures for wool threads. Strengthening and protection toward UV irradiation damages are exploited.

Optical and electron microscopy showed that halloysite nanotubes can be glued on the surface of wool fiber and the scales are acting as an anchoring site of the threads. Colorimetric analysis demonstrated that the total colour differences between standard sample and treated sample is never beyond the limits of human eyes detection. The composition of the consolidant dispersion plays a role and a Hal:keratin mass ratio of

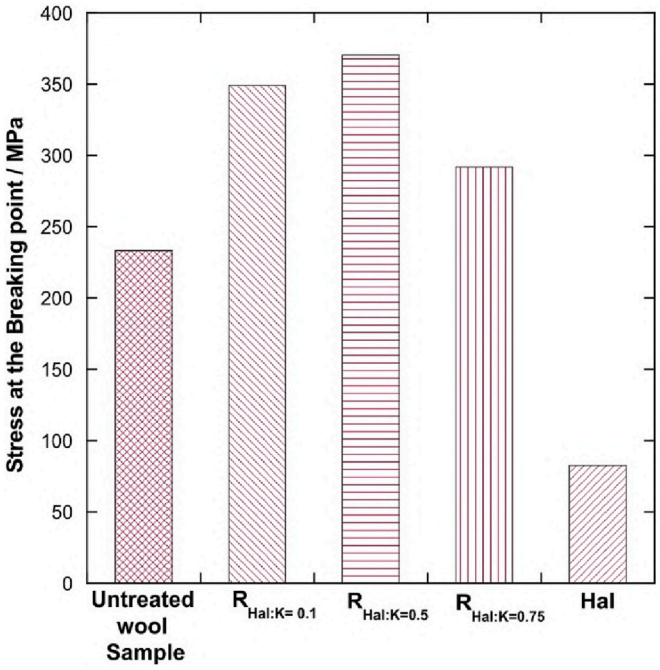

Fig. 7. Stress at breaking point (MPa) of wool yarns wool samples after UV-irradiation.

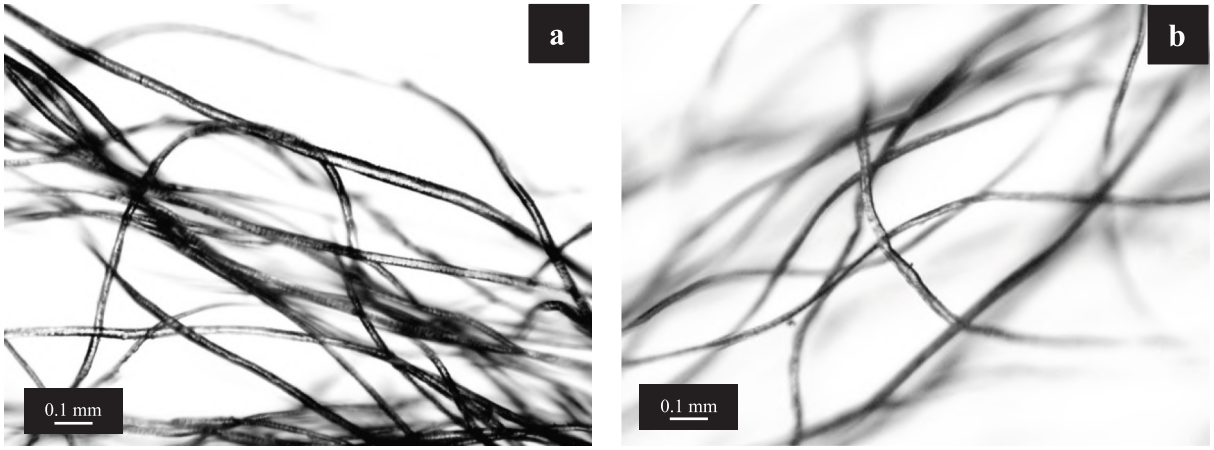

Fig. 6. Optical Microscope images of wool yarns wool sample treated with Hal/Keratn dispersion ($R_{Hal:K} = 0.5$) before (a) and after (b) UV exposure.

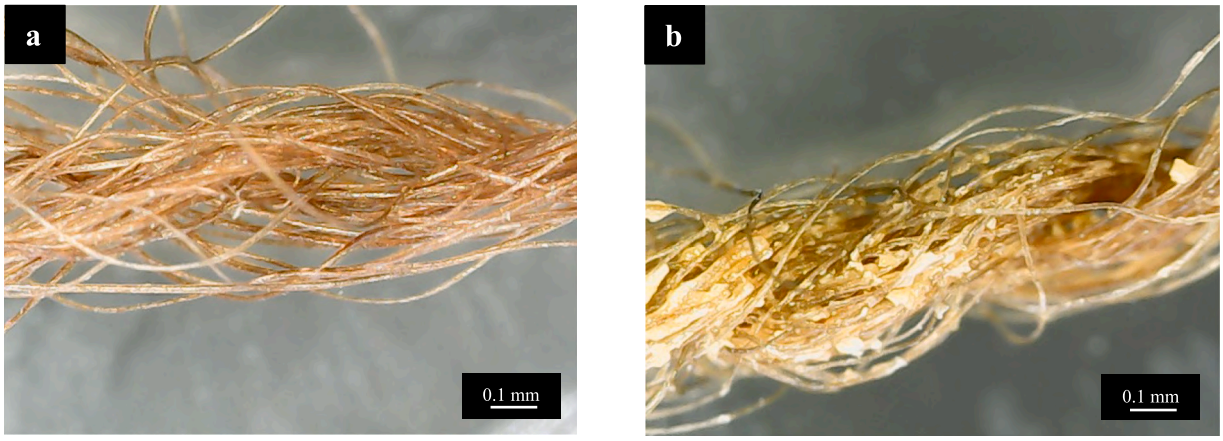

Fig. 8. Optical Microscope images of historical yarn before (a) and after (b) the treatment.

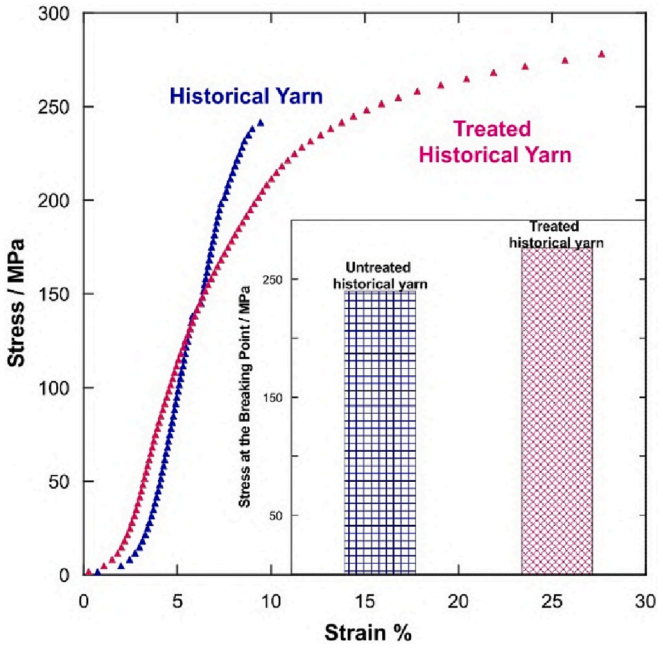

Fig. 9. Stress vs Strain Curves of historical yarn before and after treatment with $R_{Hal:K} = 0.5$. Stress at breaking is provided in the inset.

Table 3
Tensile properties of historical wool threads samples before and after treatment.

Sample	Maximum elongation (%)	Stress breaking point (MPa)	Yield Point (%)
Untreated historical yarn	9.4 ± 0.6	240 ± 16	7.8 ± 0.4
Treated historical yarn	27.6 ± 1.9	276.6 ± 19	11.5 ± 0.5

0.5 shows in the best tensile and photo-protective performances. The prospective results from treatment of contemporary wool threads samples were confirmed on a damaged wool yarn from a Flemish tapestry (Sixteenth Century).

In conclusion, the proposed protocol for wool treatment combines the capacity of Keratin to create a film as a reinforcing coating with a fully compatible chemical composition of wool threads sample, and the halloysite nanotubes ability to increase mechanical resistance and UV shielding.

CRediT authorship contribution statement

Maria Rita Caruso: Investigation, Data curation, Writing – original draft. **Giuseppe Cavallaro:** Writing – review & editing, Validation. **Stefana Milioto:** Funding acquisition, Resources. **Giuseppe Lazzara:** Conceptualization, Supervision.

Declaration of Competing Interest

None.

Data availability

Data will be made available on request.

Acknowledgments

The work was financially supported by FFR 2023, PON "Research and Innovation" 2014-2020, Asse IV "Istruzione e ricerca per il recupero", all'Azione IV.5 "Dottorati su tematiche green" DM 1061/2021 and University of Palermo. We thank "Impresa Scancarello srl" (Palermo, Italy) and Giacomo Mirto for providing the samples from the Flemish tapestry.

Appendix A. Supplementary data

Supplementary data to this article can be found online at https://doi.org/10.1016/j.clay.2023.106930.

References

Aghajani-Memar, S., Mohammadkazemi, F., Kermanian, H., Hamedi, S., 2022. Synergistic effect of bacterial cellulose and halloysite nanotubes on the properties of the sodium caseinate-based nanobiocomposites. Appl. Clay Sci. 222, 106493 https://doi.org/10.1016/j.clay.2022.106493.

Alcalá, S., Baglioni, M., Alderson, S., Neiman, M., Tallio, S.C., Giorgi, R., 2022. The use of nanostructured fluids for the removal of polymer coatings from a Nuxalk monumental carving – exploring the cleaning mechanism. J. Cult. Herit. 55, 18–29. https://doi.org/10.1016/j.culher.2022.02.002.

Baglioni, M., Poggi, G., Chelazzi, D., Baglioni, P., 2021. Advanced Materials in Cultural Heritage Conservation. Molecules 26, 3967. https://doi.org/10.3390/molecules26133967.

Bertolino, V., Cavallaro, G., Milioto, S., Lazzara, G., 2020. Polysaccharides/Halloysite nanotubes for smart bionanocomposite materials. Carbohydr. Polym. 245, 116502 https://doi.org/10.1016/j.carbpol.2020.116502.

Boccalon, E., Sassi, P., Pioppi, L., Ricci, A., Marinozzi, M., Gorrasi, G., Nocchetti, M., 2022. Onion skin extract immobilized on Halloysite-layered double hydroxide filler as active pH indicator for food packaging. Appl. Clay Sci. 227, 106592 https://doi.org/10.1016/j.clay.2022.106592.

Caruso, M.R., Lisuzzo, L., Cavallaro, G., Mirto, G., Milioto, S., Lazzara, G., 2022. Thermal and Mechanical Characterization of Yarn Samples from Flemish Tapestry of the

Sixteenth Century. Molecules 27, 8450. https://doi.org/10.3390/molecules27238450.
Cavallaro, G., Milioto, S., Nigamatzyanova, L., Akhatova, F., Fakhrullin, R.F., Lazzara, G., 2019. Pickering emulsion gels based on halloysite nanotubes and ionic biopolymers: properties and cleaning action on marble surface. ACS Appl. Nano Mater. https://doi.org/10.1021/acsanm.9b00487.
Cavallaro, G., Milioto, S., Konnova, S., Fakhrullina, G., Akhatova, F., Lazzara, G., Fakhrullin, R., Lvov, Y., 2020a. Halloysite/Keratin Nanocomposite for Human Hair Photoprotection Coating. ACS Appl. Mater. Interfaces 12, 24348–24362. https://doi.org/10.1021/acsami.0c05252.
Cavallaro, G., Milioto, S., Lazzara, G., 2020b. Halloysite Nanotubes: Interfacial Properties and applications in Cultural Heritage. Langmuir 36, 3677–3689. https://doi.org/10.1021/acs.langmuir.0c00573.
Cavallaro, G., Caruso, M.R., Milioto, S., Fakhrullin, R., Lazzara, G., 2022. Keratin/alginate hybrid hydrogels filled with halloysite clay nanotubes for protective treatment of human hair. Int. J. Biol. Macromol. 222, 228–238. https://doi.org/10.1016/j.ijbiomac.2022.09.170.
Chen, B., Xing, Y., Yu, W., Liu, H., 2018. Wool keratin and silk sericin composite films reinforced by molecular network reconstruction. J. Mater. Sci. 53, 5418–5428. https://doi.org/10.1007/s10853-017-1909-5.
Degano, I., Biesaga, M., Colombini, M.P., Trojanowicz, M., 2011. Historical and archaeological textiles: an insight on degradation products of wool and silk yarns. J. Chromatogr. A 1218, 5837–5847. https://doi.org/10.1016/j.chroma.2011.06.095.
Dei, L., Andrina, E., Cialli, O., Salvini, A., Pizzo, B., Carretti, E., 2023. A new smart material constituted of Funori and ca(OH)2 nanocrystals: Implications in cultural heritage conservation. Mater. Lett. 333, 133558 https://doi.org/10.1016/j.matlet.2022.133558.
Fakhrullin, R.F., Lvov, Y.M., 2016. Halloysite clay nanotubes for tissue engineering. Nanomedicine 11, 2243–2246. https://doi.org/10.2217/nnm-2016-0250.
Feng, Y., Zhou, X., Yang, J., Gao, X., Yin, L., Zhao, Y., Zhang, B., 2020. Encapsulation of Ammonia Borane in Pd/Halloysite Nanotubes for Efficient thermal Dehydrogenation. ACS Sustain. Chem. Eng. 8, 2122–2129. https://doi.org/10.1021/acssuschemeng.9b04480.
Feng, Y., Luo, X., Wu, F., Liu, H., Liang, E., He, R.-R., Liu, M., 2022. Systematic studies on blood coagulation mechanisms of halloysite nanotubes-coated PET dressing as superior topical hemostatic agent. Chem. Eng. J. 428, 132049 https://doi.org/10.1016/j.cej.2021.132049.
Feng, Y., He, Y., Lin, X., Xie, M., Liu, M., Lvov, Y., 2023. Assembly of Clay Nanotubes on Cotton Fibers Mediated by Biopolymer for Robust and High-Performance Hemostatic Dressing. Advanced Healthcare Materials 12, 2202265. https://doi.org/10.1002/adhm.202202265.
Giannelli, M., Barbalinardo, M., Riminucci, A., Belvedere, K., Boccalon, E., Sotgiu, G., Corticelli, F., Ruani, G., Zamboni, R., Aluigi, A., Posati, T., 2021. Magnetic keratin/hydrotalcites sponges as potential scaffolds for tissue regeneration. Appl. Clay Sci. 207, 106090 https://doi.org/10.1016/j.clay.2021.106090.
Giorgi, R., Dei, L., Ceccato, M., Schettino, C., Baglioni, P., 2002. Nanotechnologies for Conservation of Cultural Heritage: Paper and Canvas Deacidification. Langmuir 18, 8198–8203. https://doi.org/10.1021/la025964d.
Gkouma, E., Gianni, E., Avgoustakis, K., Papoulis, D., 2021. Applications of halloysite in tissue engineering. Appl. Clay Sci. 214, 106291 https://doi.org/10.1016/j.clay.2021.106291.
Gorrasi, G., Bugatti, V., Ussia, M., Mendichi, R., Zampino, D., Puglisi, C., Carroccio, S.C., 2018. Halloysite nanotubes and thymol as photo protectors of biobased polyamide 11. Polym. Degrad. Stab. 152, 43–51. https://doi.org/10.1016/j.polymdegradstab.2018.03.015.
Hoang-Minh, T., Le, T.L., Kasbohm, J., Gieré, R., 2010. UV-protection characteristics of some clays. Appl. Clay Sci. 48, 349–357. https://doi.org/10.1016/j.clay.2010.01.005.
Lisuzzo, L., Caruso, M.R., Cavallaro, G., Milioto, S., Lazzara, G., 2021a. Hydroxypropyl Cellulose Films Filled with Halloysite Nanotubes/Wax Hybrid Microspheres. Ind. Eng. Chem. Res. 60, 1656–1665. https://doi.org/10.1021/acs.iecr.0c05148.
Lisuzzo, L., Cavallaro, G., Milioto, S., Lazzara, G., 2021b. Halloysite nanotubes filled with MgO for paper reinforcement and deacidification. Appl. Clay Sci. 213, 106231 https://doi.org/10.1016/j.clay.2021.106231.
Lisuzzo, L., Hueckel, T., Cavallaro, G., Sacanna, S., Lazzara, G., 2021c. Pickering Emulsions based on Wax and Halloysite Nanotubes: an Ecofriendly Protocol for the Treatment of Archeological Woods. ACS Appl. Mater. Interfaces 13, 1651–1661. https://doi.org/10.1021/acsami.0c20443.
Liu, M., Wu, C., Jiao, Y., Xiong, S., Zhou, C., 2013. Chitosan-halloysite nanotubes nanocomposite scaffolds for tissue engineering. J. Mater. Chem. B 1, 2078–2089. https://doi.org/10.1039/C3TB20084A.
Liu, Y., Zhang, J., Guan, H., Zhao, Y., Yang, J.-H., Zhang, B., 2018. Preparation of bimetallic Cu-Co nanocatalysts on poly (diallyldimethylammonium chloride) functionalized halloysite nanotubes for hydrolytic dehydrogenation of ammonia borane. Appl. Surf. Sci. 427, 106–113. https://doi.org/10.1016/j.apsusc.2017.08.171.
Lo Nostro, P., Fratoni, L., Ninham, B.W., Baglioni, P., 2002. Water Absorbency by Wool Fibers: Hofmeister effect. Biomacromolecules 3, 1217–1224. https://doi.org/10.1021/bm0255692.
Monteiro, A., Jarrais, B., Rocha, I.M., Pereira, C., Pereira, M.F.R., Freire, C., 2014. Efficient immobilization of montmorillonite onto cotton textiles through their functionalization with organosilanes. Appl. Clay Sci. 101, 304–314. https://doi.org/10.1016/j.clay.2014.08.019.
Panchal, A., Fakhrullina, G., Fakhrullin, R., Lvov, Y., 2018. Self-assembly of clay nanotubes on hair surface for medical and cosmetic formulations. Nanoscale 10, 18205–18216. https://doi.org/10.1039/C8NR05949G.
Pramualkijja, W., Jiratumnukul, N., 2022. The preparation of hydrophobic hybrid film coatings from siloxane-modified polyacrylate associated with nano-fumed silica and organo-modified clay. J. Coat. Technol. Res. 19, 1467–1492. https://doi.org/10.1007/s11998-022-00621-1.
Rahman, N., Scott, F.H., Lvov, Y., Stavitskaya, A., Akhatova, F., Konnova, S., Fakhrullina, G., Fakhrullin, R., 2021. Clay Nanotube Immobilization on Animal Hair for Sustained Anti-Lice Protection. Pharmaceutics 13, 1477. https://doi.org/10.3390/pharmaceutics13091477.
Sadjadi, S., 2020. Halloysite-based hybrids/composites in catalysis. Appl. Clay Sci. 189, 105537 https://doi.org/10.1016/j.clay.2020.105537.
Sadjadi, S., Malmir, M., Heravi, M.M., Kahangi, F.G., 2018. Biocompatible starch-halloysite hybrid: an efficient support for immobilizing Pd species and developing a heterogeneous catalyst for ligand and copper free coupling reactions. Int. J. Biol. Macromol. 118, 1903–1911. https://doi.org/10.1016/j.ijbiomac.2018.07.053.
Samal, S., Blanco, I., 2021. Investigation of Dispersion, Interfacial Adhesion of Isotropic and Anisotropic Filler in Polymer Composite. Appl. Sci. 11, 8561. https://doi.org/10.3390/app11188561.
Vasileiadou, A., Karapanagiotis, I., Zotou, A., 2019. UV-induced degradation of wool and silk dyed with shellfish purple. Dyes Pigments 168, 317–326. https://doi.org/10.1016/j.dyepig.2019.04.068.
Wong, L.W., Pasbakhsh, P., Cheng, W.T., Goh, C.B.S., Tan, J.B.L., 2023. One-pot synthesis of injectable self-healing thermoresponsive halloysite nanotube-reinforced nanocomposite hydrogels for tissue engineering. Appl. Clay Sci. 232, 106812 https://doi.org/10.1016/j.clay.2022.106812.
Yang, X., Cai, J., Chen, L., Cao, X., Liu, H., Liu, M., 2021. Green detergent made of halloysite nanotubes. Chem. Eng. J. 425, 130623 https://doi.org/10.1016/j.cej.2021.130623.
Yu, T., Swientoniewski, L.T., Omarova, M., Li, M.-C., Negulescu, I.I., Jiang, N., Darvish, O.A., Panchal, A., Blake, D.A., Wu, Q., Lvov, Y.M., John, V.T., Zhang, D., 2019. Investigation of Amphiphilic Polypeptoid-Functionalized Halloysite Nanotubes as Emulsion Stabilizer for Oil spill Remediation. ACS Appl. Mater. Interfaces 11, 27944–27953. https://doi.org/10.1021/acsami.9b08623.
Zhang, X., Guo, Y., Li, W., Zhang, J., Wu, H., Mao, N., Zhang, H., 2021. Magnetically Recyclable Wool Keratin Modified Magnetite Powders for Efficient Removal of Cu2+ Ions from Aqueous Solutions. Nanomaterials 11, 1068. https://doi.org/10.3390/nano11051068.
Zhao, X., Zhou, C., Liu, M., 2020. Self-assembled structures of halloysite nanotubes: towards the development of high-performance biomedical materials. J. Mater. Chem. B 8, 838–851. https://doi.org/10.1039/C9TB02460C.